arXiv:1609.06631v1 [hep-ex] 21 Sep 2016

Measurement of the running of the fine structure constant below 1 GeV with the KLOE Detector

The KLOE-2 Collaboration

A. Anastasi [e,d], D. Babusci [d], G. Bencivenni [d], M. Berlowski [u], C. Bloise [d], F. Bossi [d], P. Branchini [r], A. Budano [q,r], L. Caldeira Balkeståhl [t], B. Cao [t], F. Ceradini [q,r], P. Ciambrone [d], F. Curciarello [e,b,ℓ], E. Czerwiński [c], G. D'Agostini [m,n], E. Dané [d], V. De Leo [r,*], E. De Lucia [d], A. De Santis [d], P. De Simone [d], A. Di Cicco [q,r], A. Di Domenico [m,n], R. Di Salvo [p], D. Domenici [d], A. D'Uffizi [d], A. Fantini [o,p], G. Felici [d], S. Fiore [s,n], A. Gajos [c], P. Gauzzi [m,n], G. Giardina [e,b], S. Giovannella [d], E. Graziani [r], F. Happacher [d], L. Heijkenskjöld [t], T. Johansson [t], D. Kamińska [c], W. Krzemien [u], A. Kupsc [t], S. Loffredo [q,r], P.A. Lukin [x], G. Mandaglio [f,g], M. Martini [d,k], M. Mascolo [d], R. Messi [o,p], S. Miscetti [d], G. Morello [d], D. Moricciani [p], P. Moskal [c], M. Papenbrock [t], A. Passeri [r], V. Patera [j,n], E. Perez del Rio [d], A. Ranieri [a], P. Santangelo [d], I. Sarra [d], M. Schioppa [h,i], M. Silarski [d], F. Sirghi [d], L. Tortora [r], G. Venanzoni [d,*], W. Wiślicki [u], M. Wolke [t]

and

F. Jegerlehner [v,w]

[a] *INFN Sezione di Bari, Bari, Italy.*

[b] *INFN Sezione di Catania, Catania, Italy.*

[c] *Institute of Physics, Jagiellonian University, Cracow, Poland.*

[d] *Laboratori Nazionali di Frascati dell'INFN, Frascati, Italy.*

[e] *Dipartimento di Scienze Matematiche e Informatiche, Scienze Fisiche e Scienze della Terra dell'Università di Messina, Messina, Italy.*

[f] *Dipartimento di Scienze Chimiche, Biologiche, Farmaceutiche ed Ambientali dell'Università di Messina, Messina, Italy.*

[g] *INFN Gruppo collegato di Messina, Messina, Italy.*

[h] *Dipartimento di Fisica dell'Università della Calabria, Rende, Italy.*

[i] *INFN Gruppo collegato di Cosenza, Rende, Italy.*

[j] *Dipartimento di Scienze di Base ed Applicate per l'Ingegneria dell'Università "Sapienza", Roma, Italy.*

[k] *Dipartimento di Scienze e Tecnologie applicate, Università "Guglielmo Marconi", Roma, Italy.*

[ℓ] *Novosibirsk State University, 630090 Novosibirsk, Russia.*

[m] *Dipartimento di Fisica dell'Università "Sapienza", Roma, Italy.*

[n] *INFN Sezione di Roma, Roma, Italy.*

[o] *Dipartimento di Fisica dell'Università "Tor Vergata", Roma, Italy.*

[p] *INFN Sezione di Roma Tor Vergata, Roma, Italy.*

[q] *Dipartimento di Matematica e Fisica dell'Università "Roma Tre", Roma, Italy.*

[r] *INFN Sezione di Roma Tre, Roma, Italy.*

[s] *ENEA UTTMAT-IRR, Casaccia R.C., Roma, Italy*

[t] *Department of Physics and Astronomy, Uppsala University, Uppsala, Sweden.*

[u] *National Centre for Nuclear Research, Warsaw, Poland.*

[v] *Institute of Physics Humboldt-University of Berlin, Berlin, Germany*

[w] *Deutsches Elektronen–Synchrotron (DESY), Platanenallee 6, D–15738 Zeuthen, Germany*

[x] *Budker Institute of Nuclear Physics, Novosibirsk, Russia*

Abstract

We have measured the running of the effective QED coupling constant $\alpha(s)$ in the time-like region $0.6 < \sqrt{s} < 0.975$ GeV with the KLOE detector at DAΦNE using the Initial State Radiation process $e^+e^- \to \mu^+\mu^-\gamma$. It represents the first measurement of the running of $\alpha(s)$ in this energy region. Our results show a more than 5σ significance of the hadronic contribution to the running of $\alpha(s)$, which is the strongest direct evidence both in time- and space-like regions achieved in a single measurement. By using the $e^+e^- \to \pi^+\pi^-$cross section measured by KLOE, the real and imaginary part of the shift $\Delta\alpha(s)$ has been extracted. By a fit of the real part of $\Delta\alpha(s)$ and assuming the lepton universality the branching ratio $BR(\omega \to \mu^+\mu^-) = (6.6 \pm 1.4_{stat} \pm 1.7_{syst}) \cdot 10^{-5}$ has been determined.

Key words: vacuum polarization, α running

* Corresponding authors
Email addresses: veronica.deleo@roma3.infn.it (V. De Leo), graziano.venanzoni@lnf.infn.it (G. Venanzoni).

1 Introduction

Precision tests of the Standard Model (SM) require an appropriate inclusion of higher order effects and the very precise knowledge of input parameters [1]. One of the basic input parameters is the effective QED coupling constant α, determined from the anomalous magnetic moment of the electron with the impressive accuracy of 0.37 parts per billion [2]. However, physics at non-zero momentum transfer requires an effective electromagnetic coupling $\alpha(s)$ [1]. The shift of the fine-structure constant from the Thomson limit to high energy involves low energy non-perturbative hadronic effects which affect the precision. These effects represent the largest uncertainty (and the main limitation) for the electroweak precision tests as the determination of $sin^2\theta_W$ at the Z pole or the SM prediction of the muon $g-2$ [3].
The QED coupling constant is predicted and observed [4, 5] to increase with rising momentum transfer (differently from the strong coupling constant α_S which decreases with rising momentum transfer), which can be understood as a result of the screening of the bare charge caused by the polarized cloud of virtual particles. The vacuum polarization (VP) effects can be absorbed in a redefinition of the fine-structure constant, making it s dependent:

$$\alpha(s) = \frac{\alpha(0)}{1 - \Delta\alpha(s)} \tag{1}$$

The shift $\Delta\alpha$(s) in terms of the the vacuum polarization function Π'_γ(s) is given by:

$$\Delta\alpha(s) = -4\pi\alpha(0)\,\mathrm{Re}\,[\Pi^{'}_{\gamma}(\mathrm{s}) - \Pi^{'}_{\gamma}(0)] \tag{2}$$

and it is the sum of the lepton (e,μ,τ) contributions, the contribution from the five quarks flavours (u,d,s,c,b) , and the contribution of the top quark (which can be neglected at low energies): $\Delta\alpha(\mathrm{s})=\Delta\alpha_{lep}(s) + \Delta\alpha^{(5)}_{had}(s) + \Delta\alpha_{top}(s)$ [1]. The leptonic contributions can be calculated with very high precision in QED by the perturbation theory [6]. However, due to the non-perturbative behaviour of the strong interaction at low energies, perturbative QCD only allows us to calculate the high energy tail of the hadronic (quark) contributions. In the lower energy region the hadronic contribution can be evaluated through a dispersion integral over the measured $e^+e^- \to$ hadrons cross-section:

$$\Delta\alpha_{had}(s) = -\Big(\frac{\alpha(0)s}{3\pi}\Big)\mathrm{Re}\int_{\mathrm{m}^2_\pi}^{\infty} \mathrm{ds}'\,\frac{\mathrm{R(s')}}{\mathrm{s'(s'-s-i\epsilon)}} \tag{3}$$

where $R(s)$ is defined as the cross section ratio $R(s) = \frac{\sigma_{tot}(e^+e^-\to\gamma*\to hadrons)}{\sigma_{tot}(e^+e^-\to\gamma*\to\mu^+\mu^-)}$.

[1] In the following we will indicate with s the momentum transfer squared of the reaction.

In this approach the dominant uncertainty in the evaluation of $\Delta\alpha$ is given by the experimental data accuracy.
In the Eq. (2) $\mathrm{Im}\,\Delta\alpha$ related to the imaginary part of the VP function Π'_γ is completely neglected, which is a good approximation in the continuum as the contributions from the imaginary part are suppressed. However, this approximation is not sufficient in the presence of resonances like the ρ meson, where the accuracy of the cross section measurements reaches the order of (or even less than) 1%, and the imaginary part should be taken into account.
In this paper we present a measurement of the running of the effective QED coupling constant α in the time-like region $0.6 < \sqrt{s} < 0.975$ GeV. The strength of the coupling constant is measured as a function of the momentum transfer of the exchanged photon $\sqrt{s} = M_{\mu\mu}$ where $M_{\mu\mu}$ is the $\mu^+\mu^-$ invariant mass. The value of $\alpha(s)$ is extracted from the ratio of the differential cross section for the process $e^+e^- \to \mu^+\mu^-\gamma(\gamma)$ with the photon emitted in the Initial State (ISR) to the corresponding cross section obtained from Monte Carlo (MC) simulation with the coupling set to the constant value $\alpha(s) = \alpha(0)$:

$$|\frac{\alpha(s)}{\alpha(0)}|^2 = \frac{d\sigma_{data}(e^+e^- \to \mu^+\mu^-\gamma(\gamma))|_{ISR}/d\sqrt{s}}{d\sigma^0_{MC}(e^+e^- \to \mu^+\mu^-\gamma(\gamma))|_{ISR}/d\sqrt{s}} \tag{4}$$

To obtain the ISR cross section, the observed cross section must be corrected for events with one or more photons in the final state (FSR). This has been done by using the PHOKHARA MC event generator, which includes next-to-leading-order ISR and FSR contributions [7]. In the following we only use events where the photon is emitted at small angles, which results in a large enhancement of the ISR with respect to the FSR contribution. From the measurement of the effective coupling constant and the dipion cross section [8], we extracted for the first time in a single experiment the real and imaginary part of $\Delta\alpha$.
The analysis has been performed by using the data collected with the KLOE detector at DAΦNE, the e^+e^- collider running at the ϕ meson mass, with a total integrated luminosity of 1.7 fb^{-1}.

2 The KLOE Detector

The KLOE detector consists of a cylindrical drift chamber (DC) [9] and an electromagnetic calorimeter (EMC) [10]. The DC has a momentum resolution of $\sigma_{p_\perp}/p_\perp \sim 0.4\%$ for tracks with polar angle $\theta > 45°$. Track points are measured in the DC with a resolution in $r-\phi$ of ~ 0.15 mm and ~ 2 mm in z. The EMC has an energy resolution of $\sigma_E/E \sim 5.7\%/\sqrt{E(GeV)}$ and an excellent time resolution of $\sigma_t \sim 54ps/\sqrt{E(GeV)} \oplus 100ps$. Calorimeter clusters are reconstructed grouping together energy deposits close in space and time. A superconducting coil provides an axial magnetic field of 0.52 T along the

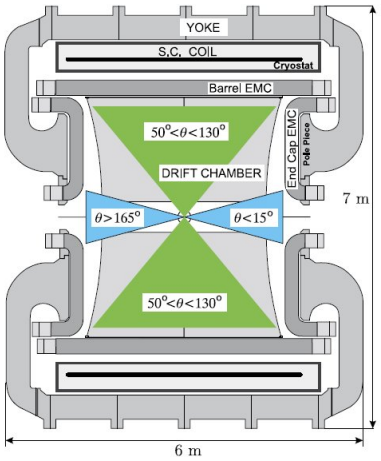

Fig. 1. Detector section with the acceptance region for the charged tracks (wide cones) and for the photon (narrow cones).

bisector of the colliding beam directions. The bisector is taken as the z axis of our coordinate system. The x axis is horizontal and the y axis is vertical, directed upwards. A cross section of the detector in the y, z plane is shown in Fig.1. The trigger uses both EMC and DC information. Events used in this analysis are triggered by two energy deposits larger than 50 MeV in two sectors of the barrel calorimeter.

2.1 Event selection

A photon and two tracks of opposite curvature are required to identify a $\mu\mu\gamma$ event. Events are selected with a (undetected) photon emitted at small angle (SA),*i.e.* within a cone of $\theta_\gamma < 15^\circ$ around the beamline (narrow cones in Fig. 1) and the two charged muons are emitted at large polar angle, $50^\circ < \theta_\mu < 130^\circ$. High statistics for the ISR signal and significant reduction of background events as $\phi \to \pi^+\pi^-\pi^0$ in which the π^0 mimics the missing momentum of the photon(s) and from the FSR radiation process, $e^+e^- \to \mu^+\mu^-\gamma_{FSR}$, are guaranteed by this selection. However, this requirement results in a kinematical suppression of events with $\sqrt{s} < 0.6$ GeV, since a highly energetic photon emitted at small angle forces the muons also to be at small angles (and thus outside the acceptance).
To avoid spiralizing tracks in the drift chamber, the reconstructed momenta must have $|p_T| > 160$ MeV or $|p_z| > 90$ MeV. This ensures good reconstruction and efficiency.
The main background reactions are given by:

- $e^+e^- \to \pi^+\pi^-\gamma(\gamma)$
- $e^+e^- \to \pi^+\pi^-\pi^0$
- $e^+e^- \to e^+e^-\gamma(\gamma)$

A particle ID estimator (PID) based on a pseudo-likelihood function ($L_{\pm}$) using time-of-flight and calorimeter information (size and shape of the energy deposit) is used to obtain separation between electrons and pions or muons. Events with both tracks satisfying $L_{\pm}$ <0 are rejected as $e^+e^-\gamma$. To identify the muons from the pions we applied mainly two cuts: the first on the track mass (M_{TRK}) variable and the second on the σ_{MTRK}, the estimated error on M_{TRK}. Assuming the presence of only one unobserved photon and that the tracks belong to particles of the same mass, M_{TRK} is computed from energy and momentum conservation. The σ_{MTRK} variable is constructed event by event with the error matrix of the fitted tracks at the point of closest approach (PCA) [11]. Cutting the high values of this variable the bad reconstructed tracks are rejected allowing a reduction of the $\pi\pi\gamma$ events contamination (shown in Fig. 2).

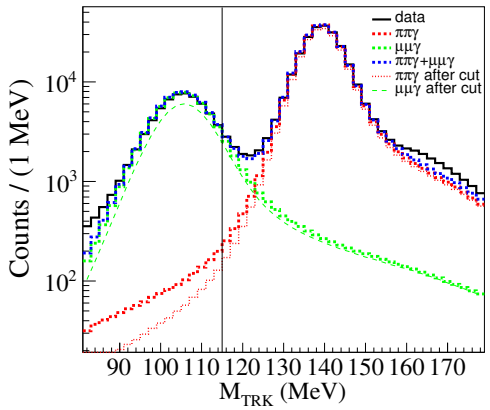

Fig. 2. $\pi\pi\gamma$ and $\mu\mu\gamma$ M_{TRK} distributions. The vertical line shows the $\mu\mu\gamma$ selection cut (M_{TRK} < 115MeV). The effect of the $\sigma_{M_{TRK}}$ cut on the two distributions is clearly visible.

Residual background is evaluated by fitting the observed M_{TRK} spectrum with a superposition of MC simulation distributions describing signal and $\pi^+\pi^-\gamma$, $\pi^+\pi^-\pi^0$ and $e^+e^-\gamma$ events. The normalization factors from signal and backgrounds are free parameters of the fit, performed for 30 intervals in s of 0.02 GeV^2 width for 0.35< s <0.95 GeV^2. Additional background from the $e^+e^- \to e^+e^-\mu^+\mu^-$ process has been evaluated using the NEXTCALIBUR MC generator [12]. The maximum contribution is 0.7% at $\sqrt{s}$=0.6 GeV. The uncertainty on this background has been taken as 50% of the total contribution and added to the systematic error. The contribution from $e^+e^- \to e^+e^-\pi^+\pi^-$ has been evaluated with the EKHARA generator [13] and found to be negligible.

The total fractional systematic uncertainty on background subtraction, obtained by adding in quadrature the uncertainties on the fit normalization parameters and the $e^+e^-\mu^+\mu^-$ residual background, ranges from 0.2% to 0.05% decreasing with s.

About $4.5 \cdot 10^6$ $\mu\mu\gamma$ events pass these selection criteria.

3 Measurement of the $\mu\mu\gamma$ cross section

The experimental ISR $\mu^+\mu^-\gamma$ cross section is obtained from the observed number of events (N_{obs}) and the background estimate (N_{bckg}) as:

$$\left.\frac{d\sigma(e^+e^- \to \mu^+\mu^-\gamma(\gamma))}{d\sqrt{s}}\right|_{ISR} = \frac{N_{obs} - N_{bkg}}{\Delta\sqrt{s}} \cdot \frac{(1-\delta_{FSR})}{\epsilon(\sqrt{s}) \cdot L} \tag{5}$$

where $(1-\delta_{FSR})$ is the correction applied to remove the FSR contribution (which increases with the energy from 0.998 at 0.605 GeV to 1.032 at 0.975 GeV), ϵ is the efficiency (see section below) and L is the integrated luminosity.
We firstly compare the $\mu^+\mu^-\gamma$ cross-section with only ISR with the corresponding NLO QED calculation from PHOKHARA generator including the VP effects.
In the upper plot of Fig. 3 the measured $\mu^+\mu^-\gamma$ cross-section as a function of $\sqrt{s}$ for both experimental (red points) and MC (blue points) data is shown. The agreement between the two cross sections is excellent. The same figure shows an interesting feature around 0.78 GeV (corresponding to the mass of the ω meson), where a small step appears in the cross section. This step behaviour is due to the $\rho - \omega$ interference to the photon propagator, as it will be shown in the following. In the lower plot the data to MC ratio is shown together with the systematic error (green band) of the order of 1%.

4 Efficiencies and systematic errors

The global efficiency, which ranges from 0.086 at 0.605 GeV to 0.27 at 0.975 GeV, has been obtained from a $\mu^+\mu^-\gamma$ events generation with PHOKHARA interfaced with the detector simulation code GEANFI [14]. It includes contributions from trigger, tracking, PID, σ_{MTRK}, M_{TRK} and acceptance.
Trigger: the trigger efficiency has been obtained from a sample of $\mu^+\mu^-\gamma$ events where a single muon satisfies the trigger requirement. Trigger response for the other muon is parameterized as a function of its momentum and direction. The efficiency as a function of s is obtained using the MC event distribution and differs from one by less than 10^{-4}, with negligible systematic error.
Tracking: the single muon track efficiency has been obtained as function of the particle momentum and polar angle by means of a high purity $\mu^+\mu^-\gamma$ sample obtained by using one muon to tag the presence of the other. The combined efficiency is about 99%, almost constant in s. The systematic un-

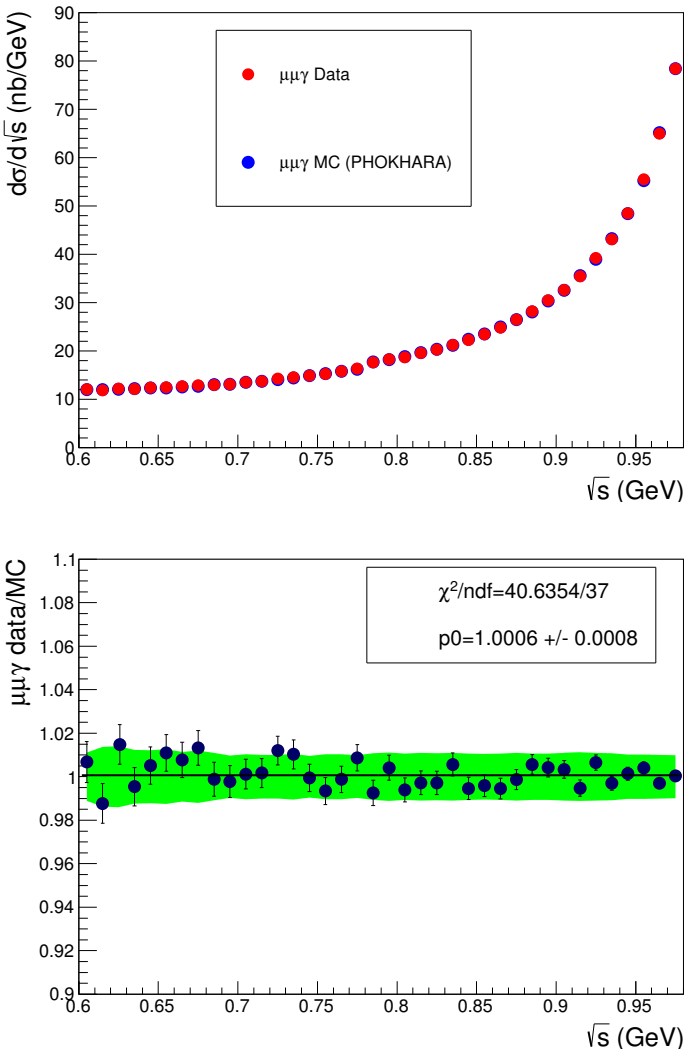

Fig. 3. Upper plot: comparison of the measured differential cross section (red points) and PHOKHARA MC prediction (blue points) of the $\mu^+\mu^-\gamma$ cross-section. Lower plot: the ratio of the two. The green band shows the systematic error.

certainty on tracking efficiency is evaluated changing the purity of the control sample and ranges from 0.3 to 0.6% as function of s.
PID: The signal efficiency due to the PID cut is more than 99.5%, as evaluated with $\mu^+\mu^-\gamma$ samples obtained both from data and Monte Carlo, with negligible systematic error.
$M_{\mathbf{TRK}}$**,** $\boldsymbol{\sigma}_{M_{\mathbf{TRK}}}$ **and Acceptance cuts**: Efficiencies are taken from MC, with systematic errors obtained as:

- The systematic uncertainty due to M_{TRK} cut has been obtained by varying the cut by one standard deviation of the mass resolution and evaluating the difference in the $\mu\mu\gamma$ spectrum. We find a fractional difference of 0.4% (constant in s) which we take as systematic error.

- The systematic uncertainty on $\sigma_{M_{\rm TRK}}$ cut has been evaluated as the maximum difference between the $\mu\mu\gamma$ normalization parameters of the background fitting procedure, obtained with standard cuts, and those obtained by shifting $\sigma_{M_{\rm TRK}}$ by $\pm 2\%$. The contribution is less than 1% in the whole energy range.

- Systematic effects due to polar angle requirements for the muons and for the photon, are estimated by varying the angular acceptance by $\pm 1^\circ$ (more than two times the resolution on the polar angle) around the nominal value. The uncertainty ranges from 0.1 to 0.6%.

Software trigger: A third level trigger is implemented to keep the physics events which are misidentified as cosmic rays. Its efficiency for $\mu\mu\gamma$ events, evaluated from an unbiased downscaled sample, is consistent with one within 10^{-3} which is taken as systematic error.
Table 1 gives the systematic errors at the ρ-peak mass value.

5 Luminosity and Radiative corrections

Large angle Bhabha scattering is used to determine the luminosity, with a reference cross section obtained with Babayaga@NLO MC event generator [15], convoluted with detector and beam conditions [16]. Two sources contribute to the systematic uncertainty in the evaluation of the luminosity:

- the theoretical accuracy of Babayaga@NLO, quoted 0.1% by the authors;
- the systematic error associated to the counting of Bhabha events which is 0.3% [16]

When extracting the running of α (see following Section), the dependence of the Bhabha cross section on the VP effect must be taken into account. By switching off the hadronic corrections to the VP, we checked that the presence of the hadronic contribution to $\Delta\alpha$ for both s and t channels in the cross section gives a 0.2% contribution which we consider as a systematic error of our measurement ($\Delta\alpha_{had}$ *dep.* in Table 1).
The uncertainty on PHOKHARA MC generator (*Rad. function H* in Table 1) is 0.5% constant in s, mostly due to missing ISR high order terms [7]. Uncertainty in the procedure to subtract the FSR contribution is 0.2% mostly due missing FSR diagrams.

Syst. errors	$\sigma_{\mu\mu\gamma}$	$\lvert\alpha(s)/\alpha(0)\rvert^2$
Trigger	$< 0.1\%$	
Tracking	s dep. (0.5% at ρ-peak)	
Particle ID	$< 0.1\%$	
Background subtraction	s dep. (0.1% at ρ-peak)	
M_{TRK}	0.4%	
σ_{MTRK}	s dep. ($< 0.1\%$ at ρ-peak)	
Acceptance	s dep. (0.3% at ρ-peak)	
Software Trigger	0.1%	
Luminosity	0.3%	
$\Delta\alpha_{had}$ dep. (Normalization)	-	0.2%
FSR treatment	0.2%	
Rad. function H	-	0.5%
Total systematic error	s dep. (0.8% at $\rho-$peak)	(1% at $\rho-$peak)

Table 1
List of systematic errors.

6 Measurement of the running of α

We use Eq.(4) and Eq.(5) in the angular region $\theta_\gamma < 15^\circ$ to extract the running of the effective QED coupling constant $\alpha(s)$. By 'undressing' the MC cross section for VP effects (*i.e. by excluding these effects*), the hadronic contribution to the photon propagator, with its characteristic $\rho-\omega$ interference structure, is clearly visibile in the data to MC ratio, as shown in Fig. 4. The prediction from Ref. [17] is also shown. While the leptonic part is obtained by perturbation theory, the hadronic contribution to $\alpha(s)$ is obtained via an evaluation in terms of a weighted average compilation of $R_{had}(s)$, based on the available experimental $e^+e^- \to$ hadrons annihilation data.

For comparison the prediction with constant coupling (*no running*) and with only lepton pairs contributing to the running of $\alpha(s)$ is given.
The value of $|\alpha(s)/\alpha(0)|^2$ with the statistical and systematic uncertainty is reported in Table 2 . As can be seen the total uncertainty is at the 1% level.
In order to evaluate the statistical significance of the hadronic contribution to the running of $\alpha(s)$, a χ^2 based statistic test for two different running hypotheses: (a) *no running*; (b) *running* due to lepton pairs only is performed.

By including statistical and systematics errors, we exclude the only-leptonic

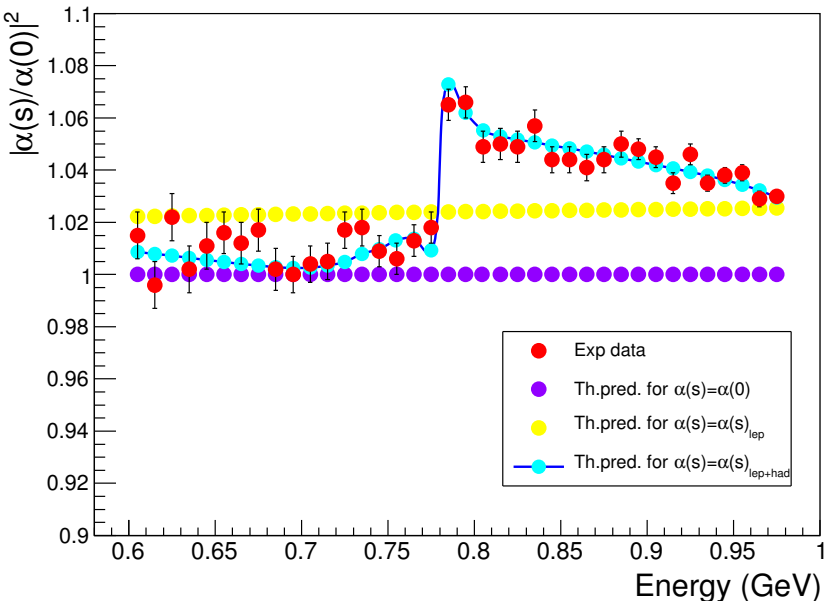

Fig. 4. The square of the modulus the running $\alpha(s)$ in units of $\alpha(0)$ compared with the prediction (provided by the `alphaQED` package [17]) as a function of the dimuon invariant mass. The red points are the KLOE data with statistical errors; the violet points are the theoretical prediction for a fixed coupling ($\alpha(s) = \alpha(0)$); the yellow points are the prediction with only virtual lepton pairs contributing to the shift $\Delta\alpha(s) = \Delta\alpha(s)_{lep}$, and finally the points with the solid line are the full QED prediction with both lepton and quark pairs contributing to the shift $\Delta\alpha(s) = \Delta\alpha(s)_{lep+had}$.

hypothesis at $6\,\sigma$ which is the strongest direct evidence ever achieved by a single experiment. Our result is also consistent with the estimate of $\Delta\alpha(s)$ of Ref. [18] with a statistical significance of 0.3 ($\chi^2/ndf = 41.2/37$).
Similar results are obtained using different $\Delta\alpha(s)$ predictions in Ref. [18, 19].

7 Extraction of Real and Imaginary part of $\Delta\alpha(s)$

In the contribution to the running of α, the imaginary part is usually neglected. This is a good approximation as the contribution from the imaginary part of $\Delta\alpha$ enters at order $O(\alpha^2)$ compared to $O(\alpha)$ for the real part, and is suppressed [20]. However, the imaginary part should be taken into account in the presence of resonances like the ρ meson, where the cross section is measured with an accuracy better than 1%.
By using the definition of the running of α (Eq. 1) the real part of the shift

$\Delta\alpha(s)$ can be expressed in terms of its imaginary part and $|\alpha(s)/\alpha(0)|^2$:

$$\mathrm{Re}\,\Delta\alpha = 1 - \sqrt{|\alpha(0)/\alpha(\mathrm{s})|^2 - (\mathrm{Im}\,\Delta\alpha)^2}. \tag{6}$$

The imaginary part of $\Delta\alpha(s)$ can be related to the total cross section $\sigma(e^+e^- \to \gamma^* \to anything)$, where the precise relation reads [3]: $\mathrm{Im}\,\Delta\alpha = -\frac{\alpha}{3}\,\mathrm{R(s)}$, with

$R(s) = \sigma_{tot}/\frac{4\pi\alpha(s)^2}{3s}$. $R(s)$ take into account leptonic and hadronic contribution $R(s) = R_{lep}(s) + R_{had}$, where the leptonic part reads:

$$R_{lep} = \sqrt{1 - \frac{4m_l^2}{s}}\left(1 + \frac{2m_l^2}{s}\right), \quad (l = e, \mu, \tau). \tag{7}$$

In the energy region around the ρ-meson we can approximate the hadronic cross section to be given by the 2π dominant contribution:

$$R_{had}(s) = \frac{1}{4}\left(1 - \frac{4m_\pi^2}{s}\right)^{\frac{3}{2}} |F_\pi^0(s)|^2 \tag{8}$$

where F_π^0 is the pion form factor deconvoluted: $|F_\pi^0(s)|^2 = |F_\pi(s)|^2 \left|\frac{\alpha(0)}{\alpha(s)}\right|^2$.

The results obtained for the 2π contribution to the imaginary part of $\Delta\alpha(s)$ by using the KLOE pion form factor measurement [8], are shown in Fig. 5 and compared with the values given by the $R_{had}(s)$ compilation of Ref. [17] using only the 2π channel, with the KLOE data removed (to avoid correlations). Table 2 gives the 2π contribution to $\mathrm{Im}\,\Delta\alpha$(s) with statistical and systematic errors.

The extraction of the $\mathrm{Re}\,\Delta\alpha$ has been performed using the Eq. (6) and it is shown in Fig. 6. The experimental data with only the statistical error included have been compared with the `alphaQED` prediction when $\mathrm{Re}\,\Delta\alpha = \mathrm{Re}\,\Delta\alpha_{\mathrm{lep}}$ (yellow points in the colour Figure) and $\mathrm{Re}\,\Delta\alpha = \mathrm{Re}\,\Delta\alpha_{\mathrm{lep+had}}$ (dots with solid line). The Re $\Delta\alpha(s)$ values with statistical and systematic errors are given in Table 2. The systematic errors include the missing hadronic contributions (3π, 4π,...) which were not included in the evaluation of $\mathrm{Im}\,\Delta\alpha$(s). As can be seen, an excellent agreement for $\mathrm{Re}\,\Delta\alpha$(s) has been obtained with the data-based compilation.

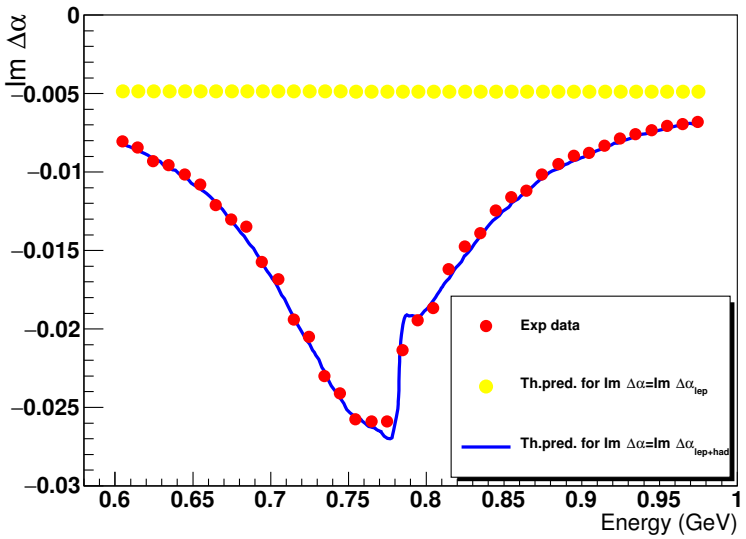

Fig. 5. $\mathrm{Im}\,\Delta\alpha$ extracted from the KLOE data compared with the values provided by `alphaQED` routine (without the KLOE data) for $\mathrm{Im}\,\Delta\alpha = \mathrm{Im}\,\Delta\alpha_{\mathrm{lep}}$ (yellow points) and $\mathrm{Im}\,\Delta\alpha = \mathrm{Im}\,\Delta\alpha_{\mathrm{lep+had}}$ only for $\pi\pi$ channels (blue solid line).

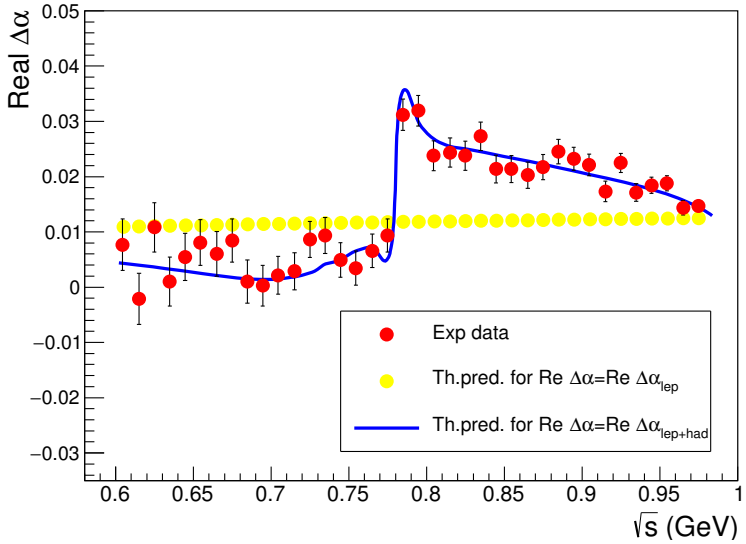

Fig. 6. $\mathrm{Re}\,\Delta\alpha$ extracted from the experimental data with only the statistical error included compared with the `alphaQED` prediction (without the KLOE data) when $\mathrm{Re}\,\Delta\alpha = \mathrm{Re}\,\Delta\alpha_{\mathrm{lep}}$ (yellow points) and $\mathrm{Re}\,\Delta\alpha = \mathrm{Re}\,\Delta\alpha_{\mathrm{lep+had}}$ (blue solid line).

$\sqrt{s}$(GeV)	$\lvert\frac{\alpha(s)}{\alpha(0)}\rvert^2$	Re $\Delta\alpha \cdot 10^{-3}$	Im $\Delta\alpha \cdot 10^{-3}$
0.605	1.015 ± 0.010±0.011	7.7±4.7±5.4	-8.09±0.08±0.03
0.615	0.996 ± 0.009±0.014	-2.2±4.6±6.9	-8.47±0.09±0.03
0.625	1.022 ± 0.009±0.014	10.7±4.5±6.8	-9.35±0.10±0.04
0.635	1.002 ± 0.009±0.012	1.0±4.4±6.1	-9.61±0.10±0.04
0.645	1.011 ± 0.009±0.012	5.4±4.3±6.0	-10.20±0.12±0.04
0.655	1.016 ± 0.009±0.013	7.9±4.2±6.1	-10.84±0.13±0.04
0.665	1.012 ± 0.008±0.011	6.0±4.1±5.6	-12.15±0.15±0.06
0.675	1.017 ± 0.008±0.012	8.3±4.0±5.9	-13.04±0.17±0.07
0.685	1.002 ± 0.008±0.011	0.9±3.9±5.4	-13.51±0.17±0.04
0.695	1.000 ± 0.007±0.010	0.2±3.7±4.9	-15.75±0.21±0.07
0.705	1.004 ± 0.007±0.010	2.1±3.4±5.1	-16.89±0.23±0.07
0.715	1.005 ± 0.007±0.010	2.7±3.3±5	-19.46±0.26±0.09
0.725	1.017 ± 0.007±0.010	8.6±3.3±4.9	-20.54±0.28±0.11
0.735	1.018 ± 0.007±0.010	9.3±3.3±5.1	-23.04±0.33±0.11
0.745	1.009 ± 0.006±0.010	4.8±3.2±4.7	-24.15±0.34±0.23
0.755	1.006 ± 0.006±0.010	3.3±3.1±5.1	-25.76±0.37±0.25
0.765	1.013 ± 0.006±0.010	6.5±3.1±5.1	-25.89±0.37±0.25
0.775	1.018 ± 0.006±0.010	9.2±3.0±4.8	-25.93±0.36±0.51
0.785	1.065 ± 0.007±0.011	31.1±3.0±4.9	-21.36±0.27±0.69
0.795	1.066 ± 0.007±0.011	31.8±3.0±5.0	-19.49±0.22±0.16
0.805	1.049 ± 0.006±0.011	23.8±2.8±5.0	-18.69±0.22±0.17
0.815	1.050 ± 0.006±0.011	24.2±2.8±5.1	-16.2±0.17±0.12
0.825	1.049 ± 0.006±0.011	23.6±2.7±5.0	-14.79±0.15±0.11
0.835	1.057 ± 0.006±0.011	27.2±2.7±5.0	-13.93±0.13±0.1
0.845	1.044 ± 0.006±0.011	21.3±2.6±5.0	-12.49±0.11±0.08
0.855	1.044 ± 0.005±0.011	21.4±2.5±4.9	-11.65±0.09±0.06
0.865	1.041 ± 0.005±0.011	20.2±2.5±5.0	-11.25±0.09±0.05
0.875	1.044 ± 0.005±0.011	21.6±2.4±5.1	-10.16±0.07±0.04
0.885	1.050 ± 0.005±0.011	24.4±2.3±4.9	-9.53±0.06±0.03
0.895	1.048 ± 0.005±0.011	23.1±2.2±5	-9.03±0.05±0.03
0.905	1.045 ± 0.004±0.011	22.0±2.1±5.1	-8.81±0.05±0.02
0.915	1.035 ± 0.004±0.011	17.2±1.9±5.3	-8.35±0.04±0.02
0.925	1.046 ± 0.004±0.011	22.3±1.8±5.1	-7.89±0.03±0.02
0.935	1.035 ± 0.003±0.011	17.0±1.7±5.1	-7.62±0.03±0.01
0.945	1.038 ± 0.003±0.010	18.3±1.5±4.8	-7.33±0.02±0.01
0.955	1.039 ± 0.003±0.010	18.8±1.4±4.8	-7.13±0.02±0.01
0.965	1.029 ± 0.003±0.010	14.2±1.3±4.8	-6.94±0.02±0.01
0.975	1.030 ± 0.002±0.010	14.6±1.1±4.7	-6.82±0.02±0.01

Table 2
$\left|\frac{\alpha(s)}{\alpha(0)}\right|^2, \mathrm{Re}\,\Delta\alpha, \mathrm{Im}\,\Delta\alpha$ values in 0.01 GeV intervals are reported; the first error is statistical, the second is systematic. The hadronic contribution to $\mathrm{Im}\,\Delta\alpha$ includes only the 2π channel from Ref. [8].

Parameter	Result from the fit	Result from the fit with $\rho-\omega$ interf.	PDG
M_ρ, MeV	775 ± 6	778 ± 7	775.26 ± 0.25
Γ_ρ, MeV	146 ± 9	147 ± 10	147 ± 0.9
M_ω, MeV	782.7 ± 1.0	783.4 ± 0.8	782.65 ± 0.12
$BR(\omega \to \mu^+\mu^-)BR(\omega \to e^+e^-)$	$(4.3 \pm 1.8) \cdot 10^{-9}$	$(4.4 \pm 1.8) \cdot 10^{-9}$	$(6.5 \pm 2.3) \cdot 10^{-9}$
χ^2/ndf	1.19	1.15	-

Table 3
Results from the fit of $\mathrm{Re}\,\Delta\alpha$ compared with the world average values (PDG [24]). Second (third) column: without (with) the $\rho-\omega$ interference. Only statistical errors are reported for the fit values.

8 Fit of $\mathrm{Re}\,\Delta\alpha$ and extraction $BR(\omega \to \mu^+\mu^-)BR(\omega \to e^+e^-)$

We fit $\mathrm{Re}\,\Delta\alpha$ by a sum of the leptonic and hadronic contributions, where the hadronic contribution is parametrized as a sum of $\rho(770)$, $\omega(782)$ and $\phi(1020)$ resonances components and a non resonant term. We use a Breit-Wigner description for the ω and ϕ resonances [3, 20, 21]:

$$\mathrm{Re}\,\Delta\alpha_{\mathrm{V}=\omega,\phi} = \frac{3\sqrt{\mathrm{BR}(\mathrm{V} \to \mathrm{e^+e^-}) \cdot \mathrm{BR}(\mathrm{V} \to \mu^+\mu^-)}}{\alpha \mathrm{M_V}} \frac{\mathrm{s}(\mathrm{s} - \mathrm{M_V^2})}{(\mathrm{s} - \mathrm{M_V^2})^2 + \mathrm{M^2\Gamma_V^2}} \quad (9)$$

where M_V and Γ_V are the mass and the total width of the mesons $V = \omega$ and ϕ. For the ρ we use a Gounaris-Sakurai parametrization $BW^{GS}_{\rho(s)}$ [22, 23] of the pion form factor, where we neglect the interference with the ω and the higher excited states of the ρ:

$$F_\pi(s) = BW^{GS}_{\rho(s)} = \frac{M_\rho^2(1 + d\Gamma_\rho/M_\rho)}{M_\rho^2 - s + f(s) - iM_\rho\Gamma_\rho(s)} \quad (10)$$

The terms d and $f(s)$ are described in Ref. [23]. As it will be shown in the following this approximation turns out to be appropriate given the limited statistics of the data. The non resonant term has been parametrized as a first-degree polynomial $p_0 + p_1\sqrt{s}$.
The following parameters have been fixed to the PDG values [24]: $\Gamma_\omega = (8.49 \pm 0.08) MeV$, $M_\phi = (1019.461 \pm 0.019) MeV$, $\Gamma_\phi = (4.266 \pm 0.031)$ MeV, and $BR(\phi \to \mathrm{e^+}\,e^-)BR(\phi \to \mu^+\mu^-) = (8.5^{+0.5}_{-0.6}) \cdot 10^{-8}$.

Results of the fit are shown in Fig. 7 and compared in Table 3 (second column) with the corresponding values from PDG [24]. Only statistical errors are reported.
The parameters of the non resonant term are consistent with zero within the statistical uncertainties: $p_0 = (2.4 \pm 4.5) \cdot 10^{-3}$, $p_1 = (-2.8 \pm 5.3) \cdot 10^{-3}$. The χ^2/ndf of the fit is $36.85/31 = 1.19$.

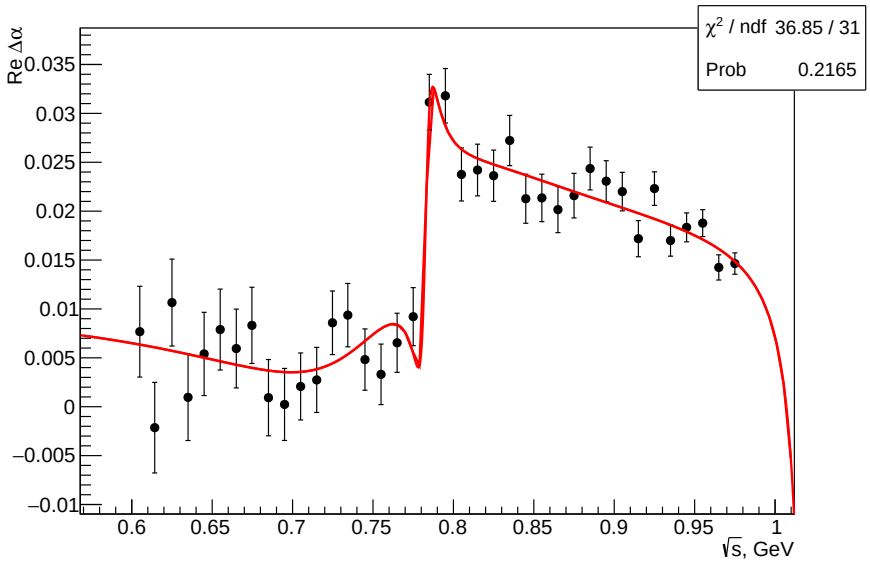

Fig. 7. Fit of the $\mathrm{Re}\,\Delta\alpha$ data. Only statistical errors are shown.

To study the effect of the $\rho - \omega$ interference in estimating $\Delta\alpha$ an additional term $\delta\frac{s}{M_\omega^2}BW_\omega(s)BW_\rho^{GS}$ has been included in the fit. Results are shown in the third column of Table 3 where we fix $|\delta| = 1.45 \cdot 10^{-3}$ and $arg\ \delta = 10.2^\circ$ [25]. As it can be seen, results with the interference term are well within the statistical uncertainties, and in the following we will use the results without the interference term.

By including the systematic errors (taking into account also the correlations of the systematic uncertainties on the parameters of the fit, and the uncertainty of the PDG values for fixed parameters) the product of the branching fractions reads:

$$BR(\omega \to \mu^+\mu^-)BR(\omega \to e^+e^-) = (4.3 \pm 1.8 \pm 2.2) \cdot 10^{-9} \qquad (11)$$

where first error statistical error and the second systematic. By multiplying for the phase space factor $\xi = \left(1 + 2\frac{m_\mu^2}{m_\omega^2}\right)\left(1 - 4\frac{m_\mu^2}{m_\omega^2}\right)^{1/2}$ and assuming lepton universality the $BR(\omega \to \mu^+\mu^-)$ can be extracted:

$$BR(\omega \to \mu^+\mu^-) = (6.6 \pm 1.4_{stat} \pm 1.7_{syst}) \cdot 10^{-5} \qquad (12)$$

compared to $BR(\omega \to \mu^+\mu^-) = (9.0 \pm 3.1) \cdot 10^{-5}$ from PDG [24].

9 Conclusions

We have measured the hadronic contribution to the running of alpha using the differential cross section $d\sigma(e^+e^- \to \mu^+\mu^-\gamma)/d\sqrt{s}$ in the region $0.6 <$

$\sqrt{s} < 0.975$ GeV, with the photon emitted in the initial state. Our results show a clear contribution of the $\rho - \omega$ resonances to the photon propagator, which results in a more than 5σ significance of the hadronic contribution to the running of $\alpha(s)$. This is the strongest direct evidence achieved in both time- and space-like regions by a single experiment. For the first time also the real and imaginary part of $\Delta\alpha(s)$ have been extracted. By a fit of the real part of $\Delta\alpha(s)$ and assuming the lepton universality the branching ratio $BR(\omega \to \mu^+\mu^-) = (6.6 \pm 1.4_{stat} \pm 1.7_{syst}) \cdot 10^{-5}$ has been obtained.

10 Acknowledgments

We thank F. Ignatov and C. M. Carloni Calame for useful discussions. We warmly thank our former KLOE colleagues for the access to the data collected during the KLOE data taking campaign. We thank the DAΦNE team for their efforts in maintaining low background running conditions and their collaboration during all data taking. We want to thank our technical staff: G.F. Fortugno and F. Sborzacchi for their dedication in ensuring efficient operation of the KLOE computing facilities; M. Anelli for his continuous attention to the gas system and detector safety; A. Balla, M. Gatta, G. Corradi and G. Papalino for electronics maintenance; M. Santoni, G. Paoluzzi and R. Rosellini for general detector support; C. Piscitelli for his help during major maintenance periods. This work was supported in part by the EU Integrated Infrastructure Initiative Hadron Physics Project under contract number RII3-CT- 2004-506078; by the European Commission under the 7th Framework Programme through the 'Research Infrastructures' action of the 'Capacities' Programme, Call: FP7-INFRASTRUCTURES-2008-1, Grant Agreement No. 227431; by the Polish National Science Centre through the Grants No. 2011/03/N/ST2/02652, 2013/08/M/ST2/00323, 2013/11/B/ST2/04245, 2014/14/E/ST2/00262, 2014/12/S/ST2/00459.

References

[1] F. Jegerlehner, J. Phys. G **29** (2003) 101.

[2] T. Aoyama, M. Hayakawa, T. Kinoshita and M. Nio, Phys. Rev. D **77** (2008) 053012.

[3] F. Jegerlehner, The anomalous magnetic moment of the muon, Springer Tracts Mod. Phys. **226** (2008) 1.

[4] A. B. Arbuzov, D. Haidt, C. Matteuzzi, M. Paganoni and L. Trentadue, Eur. Phys. J. C **34** (2004) 267.

[5] G. Abbiendi *et al.* [OPAL Collaboration], Eur. Phys. J. C **45** (2006) 1; M. Acciarri *et al.* [L3 Collaboration], Phys. Lett. B **476** (2000) 40; S. Odaka *et al.* [VENUS Collaboration], Phys. Rev. Lett. **81** (1998) 2428; I. Levine *et al.* [TOPAZ Collaboration], Phys. Rev. Lett. **78** (1997) 424.

[6] M. Steinhauser, Phys. Lett. B **429** (1998) 158.

[7] H. Czyz, A. Grzelinska, J. H. Kuhn and G. Rodrigo, Eur. Phys. J. C **39** (2005) 411; H. Czyz, A. Grzelinska, J. H. Kuhn and G. Rodrigo, Eur. Phys. J. C **33** (2004) 333; H. Czyz, A. Grzelinska, J. H. Kuhn and G. Rodrigo, Eur. Phys. J. C **27** (2003) 563; G. Rodrigo, H. Czyz, J. H. Kuhn and M. Szopa, Eur. Phys. J. C **24** (2002) 71.

[8] D. Babusci *et al.* [KLOE Collaboration], Phys. Lett. B **720** (2013) 336.

[9] M. Adinolfi *et al.*, Nucl. Instrum. Meth. A **488** (2002) 51.

[10] M. Adinolfi *et al.*, Nucl. Instrum. Meth. A **482** (2002) 364.

[11] D. Babusci *et al.* [KLOE-2 Collaboration], Phys. Lett. B **736** (2014) 459.

[12] F. A. Berends, C. G. Papadopoulos and R. Pittau, Comput. Phys. Commun. **136** (2001) 148.

[13] H. Czyz and E. Nowak-Kubat, Phys. Lett. B **634** (2006) 493; H. Czyz and E. Nowak, Acta Phys. Polon. B **34** (2003) 5231.

[14] F. Ambrosino *et al.*, Nucl. Instrum. Meth. A **534** (2004) 403.

[15] G. Balossini, C. M. Carloni Calame, G. Montagna, O. Nicrosini and F. Piccinini, Nucl. Phys. B **758** (2006) 227; C. M. Carloni Calame, C. Lunardini, G. Montagna, O. Nicrosini and F. Piccinini, Nucl. Phys. B **584** (2000) 459.

[16] F. Ambrosino *et al.* [KLOE Collaboration], Eur. Phys. J. C **47** (2006) 589.

[17] F. Jegerlehner, `alphaQED` package [version April 2012] `http://www-com.physik.hu-berlin.de/~fjeger/alphaQED.tar.gz`; see also F. Jegerlehner, Nuovo Cim. C **034S1** (2011) 31; Nucl. Phys. Proc. Suppl. **162** (2006) 22.

[18] `http://cmd.inp.nsk.su/~ignatov/vpl`.

[19] K. Hagiwara, A. D. Martin, D. Nomura and T. Teubner, Phys. Lett. B **649** (2007) 173; K. Hagiwara, A. D. Martin, D. Nomura and T. Teubner, Phys. Rev. D **69** (2004) 093003; K. Hagiwara, R. Liao, A. D. Martin, D. Nomura and T. Teubner, J. Phys. G **38** (2011) 085003.

[20] S. Actis et al. Eur. Phys. J. C **66** (2010) 585.

[21] S. Iwao and M. Shako, Lett. Nuovo Cim. **9** (1974) 693.

[22] G. J. Gounaris and J. J. Sakurai, Phys. Rev. Lett. **21** (1968) 244.

[23] R. R. Akhmetshin *et al.* [CMD-2 Collaboration], Phys. Lett. B **527** (2002) 161.

[24] K. A. Olive *et al.* [Particle Data Group Collaboration], Chin. Phys. C **38** (2014) 090001.

[25] G. Mandaglio *et al.*, G. Mandaglio [KLOE-2 Collaboration], Nucl. Part. Phys. Proc. **260** (2015) 87.